CHAPTER III

RESULTS AND DISCUSSION

3.1 Monomer Synthesis

The most widely used synthetic route to 3,4-dialkoxythiophenes was the double Williamson ether synthesis from 3,4-dihydroxythiophene, as illustrated the five step route in **Scheme 3.1**.

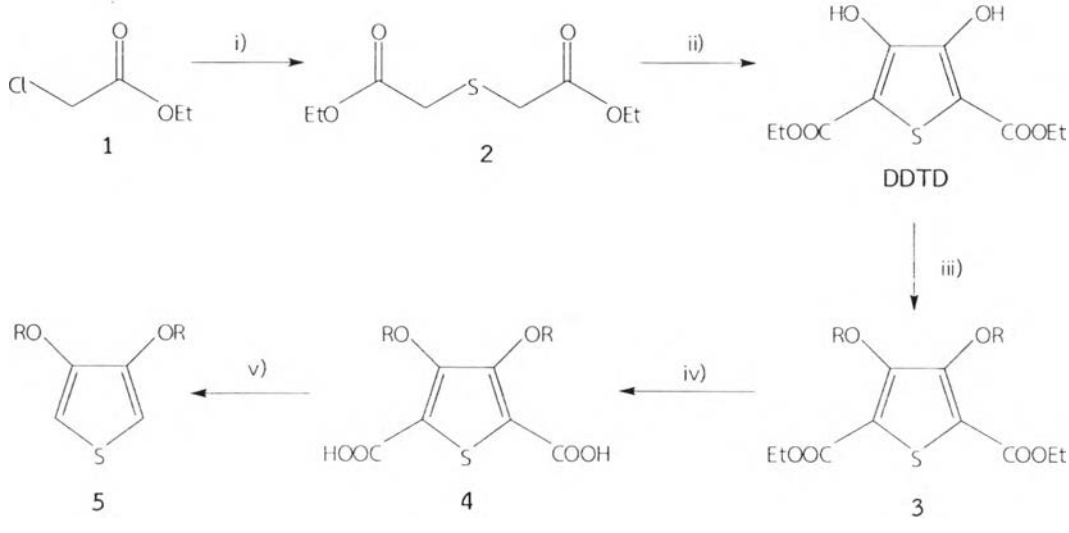

Scheme 3.1 *Reagents and conditions:* i) $Na_2S.9H_2O$, acetone, 60 °C, 3 h; ii) NaOEt, 30 m, $(CO_2Et)_2$, reflux 3 h; iii) Alkyl halide reagent (R-X), base, reflux; iv) NaOH, EtOH, reflex 10 h; v) Cu_2O, quinoline, 150 °C, 20 h.

3.1.1 Diethyl thioglycolate 2

Ethyl chloroacetate **1** was obtained from the reaction of chloroacetyl chloride and EtOH. This reaction underwent the bimolecular nucleophilic acyl substitution. The presence of quartet and triplet signals of the newly added ethyl group appeared at 4.24 and 1.29 ppm in the ^{1}H NMR spectrum **(Figure A.1, Appendix A)** and 62.2 and 14.0 ppm in the ^{13}C NMR spectrum **(Figure A.2, Appendix A)**.

The solution of ethyl chloroacetate **1** in acetone was treated through the S_N2 reaction with sodium sulfide [34]. Compound **2** was obtained in 45% yield. The ^{1}H NMR spectrum showed a singlet methylene peak at 3.37 ppm, and the quartet and

triplet signals of the ethyl group at 4.19 and 1.28 ppm, respectively **(Figure A.3, Appendix A)**. The carbonyl carbon in the ^{13}C NMR spectrum appeared at 169.5 ppm **(Figure A.4, Appendix A)**.

3.1.2 Diethyl 3,4-dihydroxythiophene-2,5-dicarboxylate (DDTD)

The synthesis of diethyl 3,4-dihydroxythiophene-2,5-dicarboxylate (DDTD) began with the Hinsberg reaction [35], which is a condensation of diethyl thioglycolate **2** with diethyl oxalate under basic condition. The mechanism is the consecutive Claisen condensation reactions to produce a diketone intermediate, which readily tautomerizes to the corresponding dihydroxythiophene **(Scheme 3.2)**.

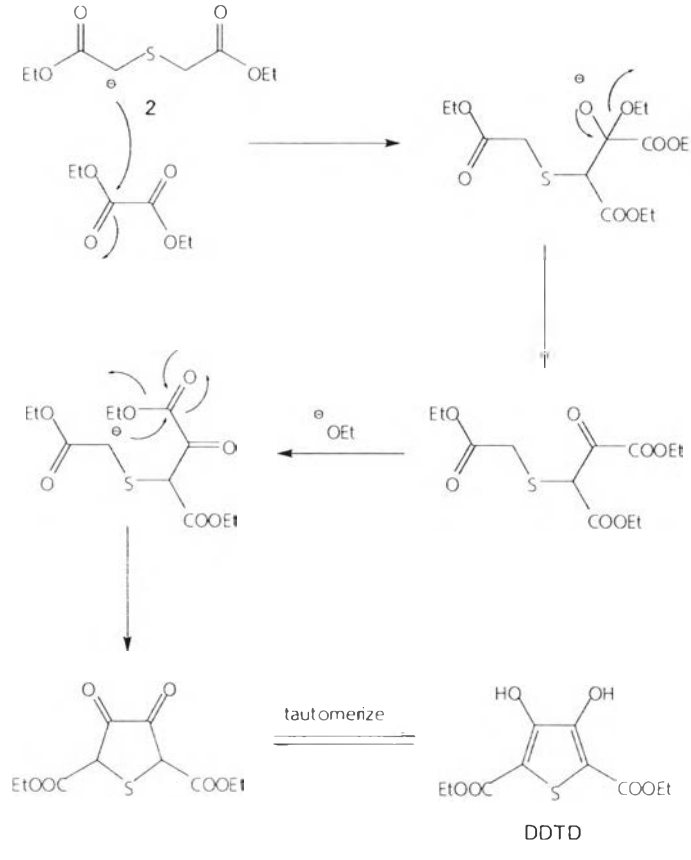

Scheme 3.2 Mechanism of Hinsberg reaction to generate DDTD

DDTD was obtained as white needle crystals in 68% yield after recrystallization in methanol. ^{1}H NMR showed a broad singlet -OH peak at 9.36 ppm **(Figure A.6, Appendix A)**. In the ^{13}C NMR spectrum, the carbonyl carbon appeared at 165.5 ppm and the two carbons of the thiophene ring were at 107.1 and 151.6

ppm **(Figure A.7, Appendix A)**. IR spectrum showed very strong broad -OH stretching appeared at 3305 cm^{-1} and the double bond region at 1690 and 1663 cm^{-1} **(Figure A.8, Appendix A)**.

3.1.3 Substitutions on DDTD

Compound **3a** was synthesized via methylations of DDTD. **(Table 3.1)** [36].

Table 3.1 Conditions for the synthesis of compound **3a**

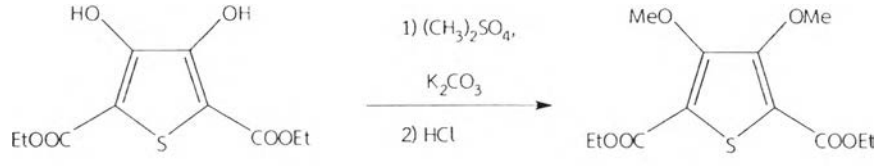

DDTD 3a

Entry	$(CH_3)_2SO_4$ (equiv)	Time (h)	Yield (%)
1	3	3	73
2	6	10	65
3	10	30	68

From **Table 3.1 (Entry 2 and 3)**, increasing the amount of dimethyl sulfate did not improve the reaction time and yield of the obtained product. Compound **3a** was structurally confirmed by the presence of the singlet methyl signal at 4.01 ppm in ^{1}H NMR spectrum **(Figure A.10, Appendix A)** and at 61.9 ppm in ^{13}C NMR spectrum **(Figure A.11, Appendix A)**. IR spectrum no longer showed strong broad band of -OH group at 3305 cm^{-1} **(Figure A.12, Appendix A)**.

Compound **3b** was synthesized in good yield via the similar double Williamson etherification under the conditions reported in the literature, using compound DDTD, 1,2-dibromoethane, Et_3N, and dry DMF as the solvent [37] **(Table 3.2)**. Changing the solvent to acetonitrile, together with increasing the equivalence of 1,2-dibromoethane and Et_3N, increased the yield of the product **(Entry 2)**. On the contrary, using mixture of solvents (DMF:CH_3CN, 2:8) worsened the result **(Entry 2 and 3)**. It is possible that part of the product may be lost during the repeated aqueous washes off the leftover DMF solvent.

Table 3.2 Conditions for the synthesis of compound **3b**

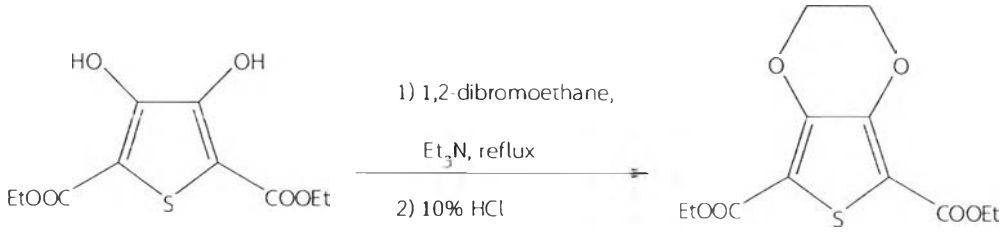

DDTD **3b**

Entry	1,2-Dibromoethane (equiv)	Et_3N (equiv)	Solvent	Time (h)	Yield (%)
1	1.3	3	DMF	24	63
2	5.5	5.5	CH_3CN	24	87
3	5.5	5.5	DMF:CH_3CN (2:8)	24	67

The obtained product **3b** was characterized by the presence of the singlet ethylene signal at 4.40 ppm in ^{1}H NMR spectrum **(Figure A.13, Appendix A)** and at 64.7 ppm in ^{13}C NMR spectrum **(Figure A.14, Appendix A)**. IR spectrum showed no strong broad band of -OH group at 3305 cm^{-1} **(Figure A.15, Appendix A)** [37].

Compound **3c** was synthesized from DDTD and epichlorohydrin obtained as yellow solid in 57% yield **(Table 3.3)** [38].

Table 3.3 Conditions for the synthesis of compound **3c**

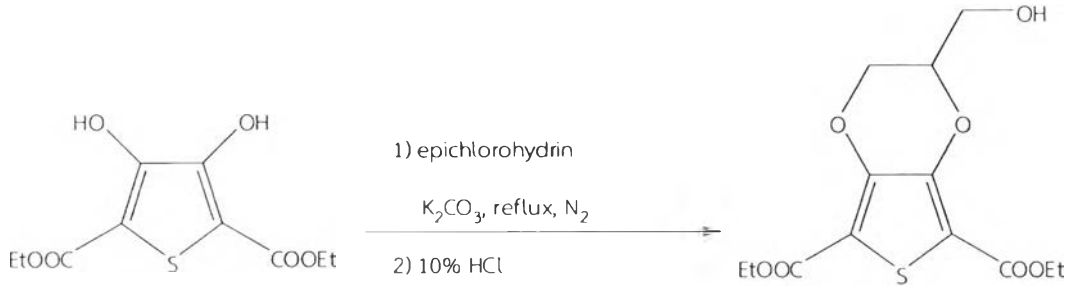

DDTD **3c**

Entry	Epichlorohydrin (equiv)	K_2CO_3 (equiv)	Time (h)	Yield (%)
1	6	2	72	57
2	6	2	96	39

Surprisingly, increase of the reaction time resulted in lower yield of the desired product **(Entry 2)**. It was assumed that **3c** was converted to a by-product from further reaction with epichlorohydrin. The signal in ^{1}H NMR spectrum at δ 9.36 ppm which corresponds to hydrogen signal of -OH groups of DDTD was absent and new multiplet signals appeared at 4.47, 4.36 and 4.27 ppm. **(Figure 17, Appendix A)**. The ^{13}C NMR spectrum matched well with the structure and that from literature **(Figure A.18, Appendix A)** [38].

3.1.4 Hydrolysis of diethylester derivatives

Compound **3a**, **3b**, and DDTD were saponified to obtain 3,4-dialkoxythiophene-2,5-dicarboxylic acid as the desired products in high yields as shown in **Table 3.4** [36]. All products gave the corresponding structural analyses by NMR and IR spectroscopy.

Table 3.4 Hydrolysis of diethylester derivatives

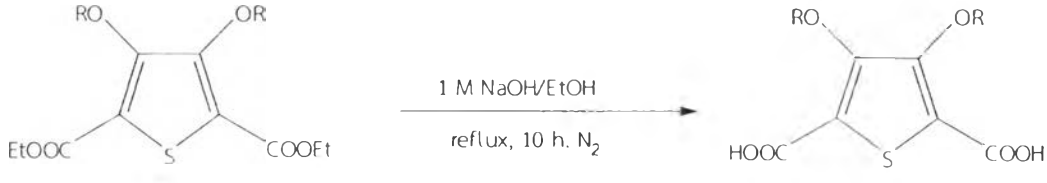

3 4

Entry	Starting material	Product	Yield (%)
1	3a	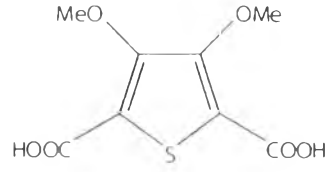 4a	80
2	3b	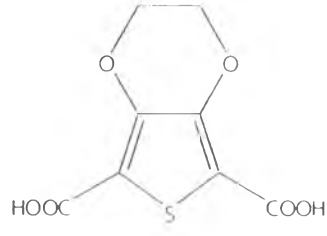 4b	96
3	DDTD	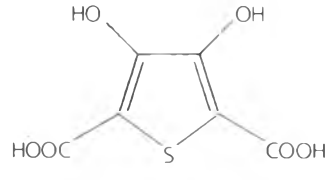 4d	98

Only **4d** was further purified by crystallization from methanol. The ^{1}H NMR and ^{13}C NMR spectra of compounds **4a**, **4b**, and **4d** were similar to those of starting materials except the absence of the signals of ethyl groups **(Figure A.20, A.23 and A.26, Appendix A)**. All compounds showed the characteristic strong carbonyl stretching peak and strong broad band of carboxyl -OH stretching in IR spectra **(Figure A.22, A.25 and A.27, Appendix A)**. Unfortunately, the expected compound **4c** could not be isolated, possibly due to the small scale of the reaction and rather high solubility of the product in water.

3.1.5 Decarboxylations of dicarboxylic acid derivatives

3,4-Dialkoxythiophenes **5** were synthesized via decarboxylations of 3,4-dialkoxythiophene-2,5-dicarboxylic acid precursors **4** using Cu_2O in quinolone [34, 36, 39]. The desired products were obtained in good yields **(Table 3.5)** except **5d**, which decomposed during column chromatography purification.

Table 3.5 Decarboxylations of the diacid compounds **4**

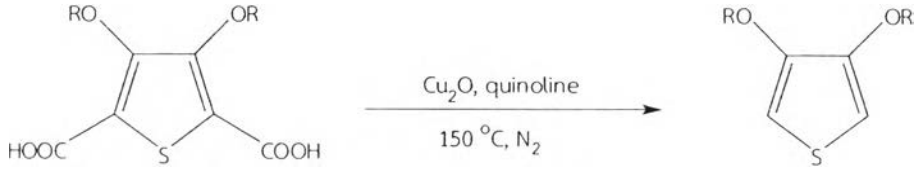

4 **5**

Entry	Starting material	Product	Yield (%)
1	**4a**	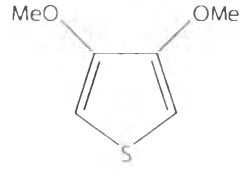 **5a**	63
2	**4b**	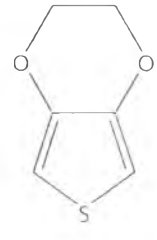 **5b** (EDOT)	70

The ^{1}H NMR and ^{13}C NMR spectra of **5a** and **5b** matched with those spectra reported in the literature [34, 36, 39] **(Figure A.29, A.30, A.32 and A.33, Appendix A)**. The ^{1}H NMR spectra showed singlet signals of α-protons of thiophene rings at 6.20 and 6.32 ppm for **5a** and **5b**, respectively. The carbonyl stretching peaks were no longer observed in their IR spectra as well. **(Figure A.31 and A.34, Appendix A)**.

3.1.6 2,3-Dihydrothieno[3,4-*b*]-1,4-dioxin-2-yl methanol (EDTM, 6)

Because of the unsuccessful diester hydrolysis, Compound **6** was instead synthesized by ether exchange between 3,4-dimethoxythiophene **5a** and glycerol using PTSA as an acid catalyst **(Table 3.6)**.

Table 3.6 Conditions for the synthesis of **6**

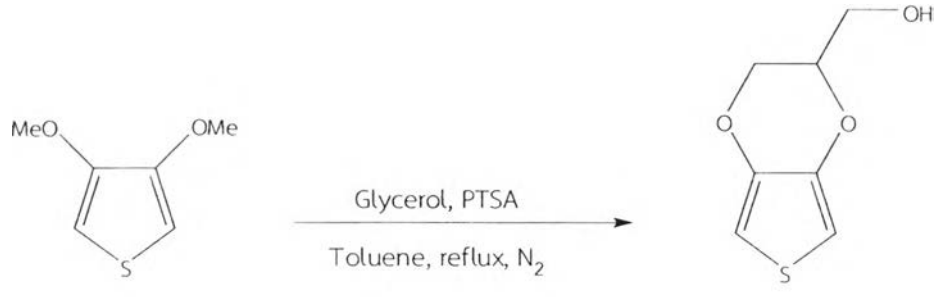

5a **6**

Entry	5a (mmol)	Glycerol (mmol)	PTSA (mmol)	Time (h)	Yield (%)
1	1	6	0.2	48	42
2	1	18	0.75	72	39
3	10	30	2	72	17

Following the procedure, compound **6** could be prepared in moderate yields. Increasing the equivalence of glycerol and PTSA with extended reaction time could not improve the product yield **(Entry 2)**. Moreover, the scale-up reaction gave even poorer product yield **(Entry 3)**. Compound **6** was characterized via ^{1}H NMR, ^{13}C NMR and IR spectra and the results matched well with those reported in the literature **(Figure A.35-A.37, Appendix A)** [38].

3.1.7 Brominations of thiophene derivatives

The α-positions of thiophene ring are generally reactive towards electrophiles or radicals, especially for electron-rich thiophenes. Following the bromination procedure by Kellogg and coworkers [25], **5b** was brominated at room temperature using *N*-bromosuccinimide (NBS) to provide **7b** in only 1-2 min according to **Scheme 3.3**.

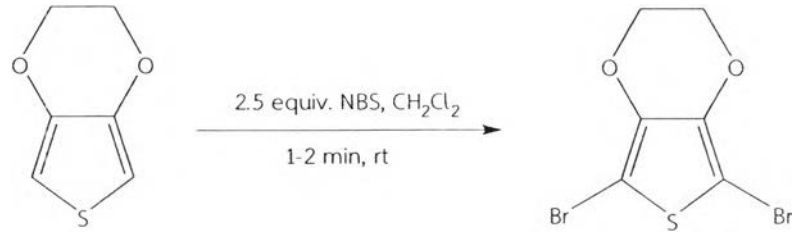

5b **7b**

Scheme 3.3 Synthesis of compound **7b**

The original synthesis of **7b** gave only moderate yield and used long reaction time. A better process was developed **here (Table 3.7)**. It was found that high yields of brominations could simply be obtained when treated with NBS in halogenated solvent at room temperature and ambient atmosphere. This condition gave pure **7b** in excellent yields **(Entry 1 and 2)**. Extension of reaction time probably degraded the product obtained and resulted in lower yield **(Entry 3)**.

Table 3.7 Conditions for synthesis of **7b**

Entry	Solvent	Time (min)	Yield (%)
1	CH_2Cl_2	1-2	98
2	$CHCl_3$	1-2	97
3	CH_2Cl_2	5	92

The product was characterized by ^{1}H NMR spectrum with the absence of a signal at δ~6.32 ppm which corresponds to the α-hydrogen signal on the thiophene ring before bromination **(Figure A.42, Appendix A)**.

The above optimal procedure was applied to other thiophene derivatives (Table 3.8).

Table 3.8 Synthesis of 2,5-dibromo-3,4-dialkoxythiophene derivatives **7**

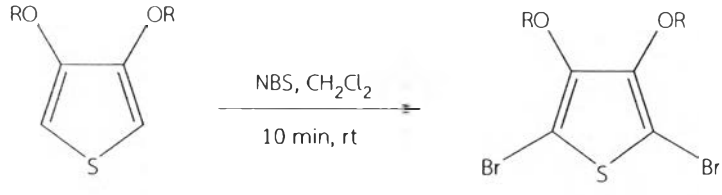

5 **7**

Entry	Starting material	Product	Yield (%)
1	**5a**	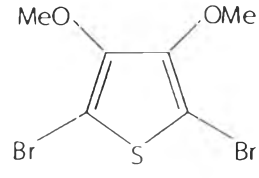 **7a**	82
2	**6**	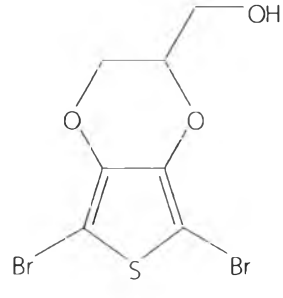 **7c**	77

For compounds **7a** and **7c**, it was observed that increasing the reaction time to 10 minutes gave higher expected yields. Slightly longer time was required probably due to less reactivity of their precursors.

3.1.8 Bromodecarboxylation of 3,4-dialkoxythiophene-2,5-dicarboxylic acid 4

The one-pot synthesis of the 2,5-dibromo-3,4-dialkoxythiophenes **7** were attempted by combining the decarboxylation and bromination reactions into one-step process as shown in **Scheme 3.4**.

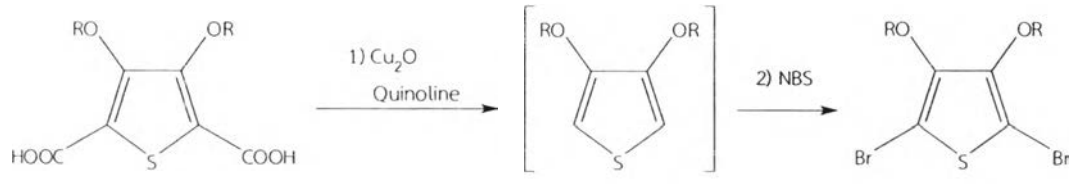

4 **5** **7**

Scheme 3.4 One pot synthesis of compound **7**

Table 3.9 Bromodecarboxylations of the diacid compounds **4**

Entry	Starting material	Product	Yield (%)
1	4a	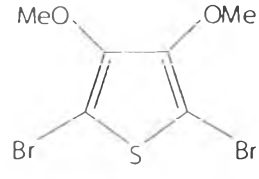 **7a**	29
2	4b	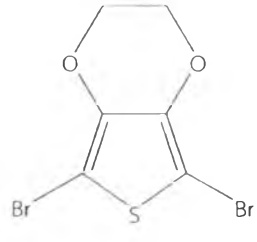 **7b**	77

Though convenient, the result of the one-pot synthesis of **7a** was inferior to that from two-step process, which gave totally 52% of product. The cause of this result may be incompletion reaction during the decarboxylation step **(Entry 1)**. On the contrary, the result of the one-pot synthesis of **7b** was superior to the separated step procedure, which gave 68% total yield from two steps **(Entry 2)**.

3.2 Preparations of template molecules

3.2.1 2,4,6-Trinitrophenol (TNP)

The *p*-Nitrophenol was nitrated with concentrated nitric acid in ice-salt bath and ambient atmosphere **(Scheme 3.5)**. After completion, compound TNP as yellow solid was obtained in 67% yield [42].

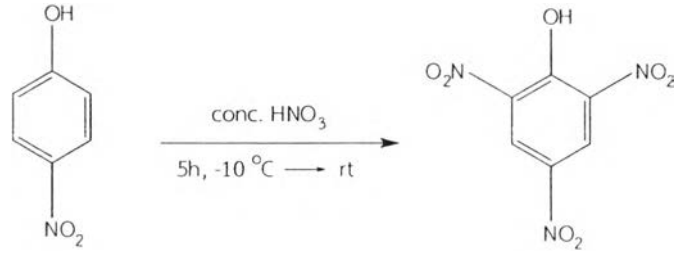

Scheme 3.5 Synthesis of 2,4,6-trinitrophenol (TNP)

The ^{1}H NMR spectrum of TNP showed the singlet signal of aromatic protons and broad signal of -OH group at 9.21 and 11.91 ppm, respectively **(Figure A.49, Appendix A)**.

3.2.2 2,4,6-Trinitrotoluene (TNT)

Compound TNT was synthesized through the nitration of toluene with fuming nitric acid. The initial mono and di-nitrations of toluene as yellow oil were obtained. Adding concentrated sulfuric acid and using heat could accelerate the reaction to get the final TNT **(Scheme 3.6)**. This light yellow solid was obtained in 74% yield [43].

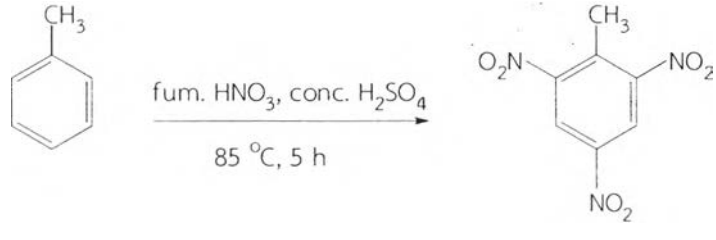

Scheme 3.6 Synthesis of 2,4,6-trinitrotoluene (TNT)

The ^{1}H NMR spectrum of TNT exhibited the singlet signal of aromatic protons and methyl group at 8.85 and 2.72 ppm, respectively **(Figure A.50, Appendix A)**

3.3 Preparation of molecularly imprinted polymers (MIPs)

Solid state polymerization (SSP) method reported by Meng and coworkers [25, 26] conveniently provided dark blue readily-doped PEDOT from simple heating of the corresponding dibromo derivatives of EDOT, **7b**. The resulted insoluble PEDOT become an ideal framework for molecular imprinting. Suitable template molecules were seemingly trapped within the cavities created during the SSP processes of the mixture of the dibromo precursors and that template. After these template molecules were removed by exhaustive Soxhlet extraction with methanol, the resultant polymers with supposedly vacant specific cavities imprinted for the removed template were obtained. The SSP process was expected to rigidly lock the arrangement of the cavities within the polymer matrix. Then dried MIPs were re-submerged in template solution and the rebinding process was monitored by UV-Vis spectroscopy. Exact experiment was repeated with a corresponding NIP in parallel with each set of study. Finally, the amount of template molecules bound to the polymers values (Q) at various sampling times of MIPs and NIPs were calculated to compare the imprinting effect [44, 45].

3.3.1 Tetraphenylporphyrin (TPP) imprinting

TPP was chosen as the first template due to its strong absorption in visible region. Its MIP was prepared from SSP of **7b** and TPP solid mixture. However, its was found that the solution of TPP in dichloromethane slowly exhibited a red shift of the absorption spectrum from 417 nm to 446 nm in the presence of the SSP-PEDOT **(Figure 3.1)**. The spectroscopic changes of TPP in dichloromethane are perhaps due to the protonation or bromination of the porphyrin core nitrogen atoms with the generated bromine in the doped PEDOT during the in situ polymerization and binding processes [46]. This absorption shift made it very difficult to quantitatively monitor the change of TPP concentration.

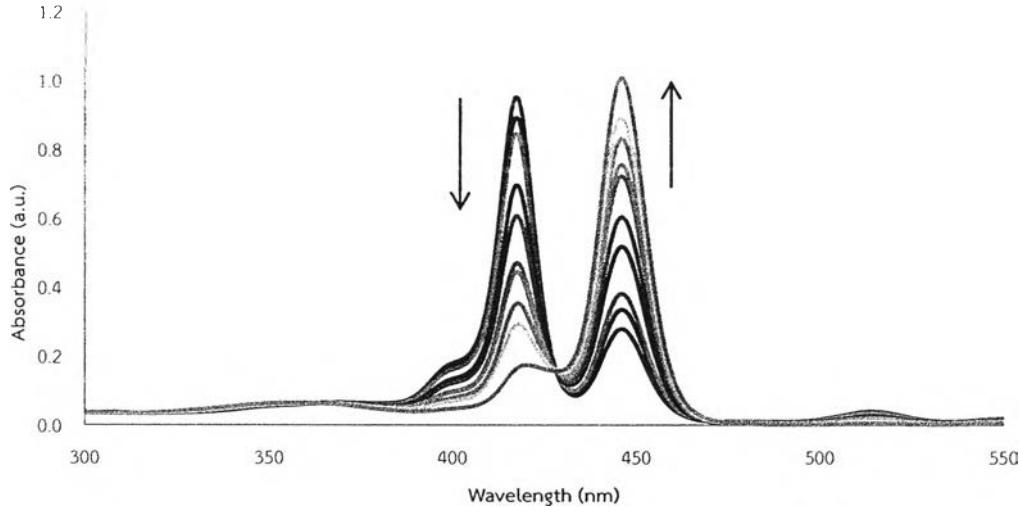

Figure 3.1 The spectroscopic changes of TPP in dichloromethane with SSP-PEDOT at various times (0-9 h)

To prove the hypothesis of interference from bromine doping agent, vacant MIP samples were dedoped with 50% solution of hydrazinium dichloride and NaOH overnight. Then the dried dedoping MIP sample was re-submerged with TPP solution in dichloromethane. Unfortunately, the same shift of absorption spectra of TPP solution in dichloromethane still occurred. Therefore, the doping agent did not involve in such shift of which cause remains unknown.

Fortunately, changing the solvent to ethyl acetate eliminated the problem. The absorption wavelength of TPP solution in ethyl acetate did not change upon mixing with doped PEDOT-MIP **(Figure 3.2)**. Hence, the concentration could be monitored at λ_{max} of 417 nm using the prepared calibration curve of TPP in this solvent. (0.36—1.68 μmol/mL) **(Figure B.3, Appendix B)**.

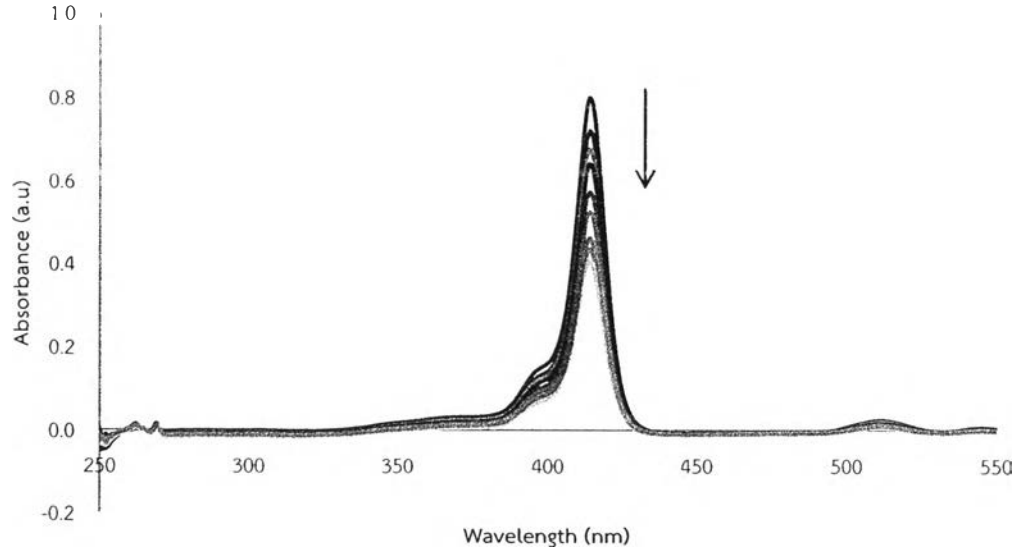

Figure 3.2 The changes in absorption spectra of TPP in ethyl acetate with SSP-PEDOT at various times (0-9 h)

In the binding experiments **(Figure 3.3)**, the concentration of TPP solution in ethyl acetate in the presence of TPP-MIPs gradually decreased with time. Similar result was disappointingly found in NIPs as well. The difference margin was rather small to impose any meaningful imprinting effect. Changing the initial concentration of TPP template solution from 1000 ppm to 2000 ppm during MIP preparation and extending the time for the binding experiment, unfortunately, did not give any significant change to the binding difference of TPP-MIP and NIP.

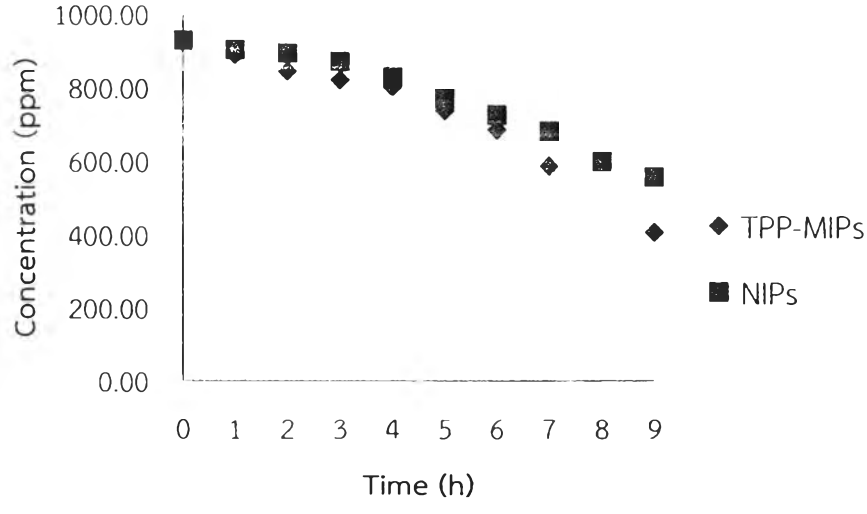

Figure 3.3 The concentrations of TPP in ethyl acetate during binding process in the presence of TPP-MIPs and NIPs at various times

It could be seen that the TPP-MIPs based on SSP-PEDOT showed only small imprinting effects. The possible reasons may be from the complications of absorption uncertainty, the still unknown reactivity of TPP with the doped polymer, and the rather large size of TPP that created large imprinted cavities that may collapse during template removal.

3.3.2 2,4,6-Trinitrophenol-molecularly imprinted polymers (TNP-MIPs)

Another binding experiment was carried out to investigate the imprinting effect using TNP as the template molecules. For TNP-MIPs, the concentrations of TNP solution in ethyl acetate gradually decreased and reached equilibrium in 8 hours. On the contrary, the concentrations of TNP solution in ethyl acetate for NIPs only marginally decreased in the beginning and later fluctuated within a narrow range, which could be considered to show no specific response to the template. The difference between the two samples was significant in this case **(Figure 3.4)**.

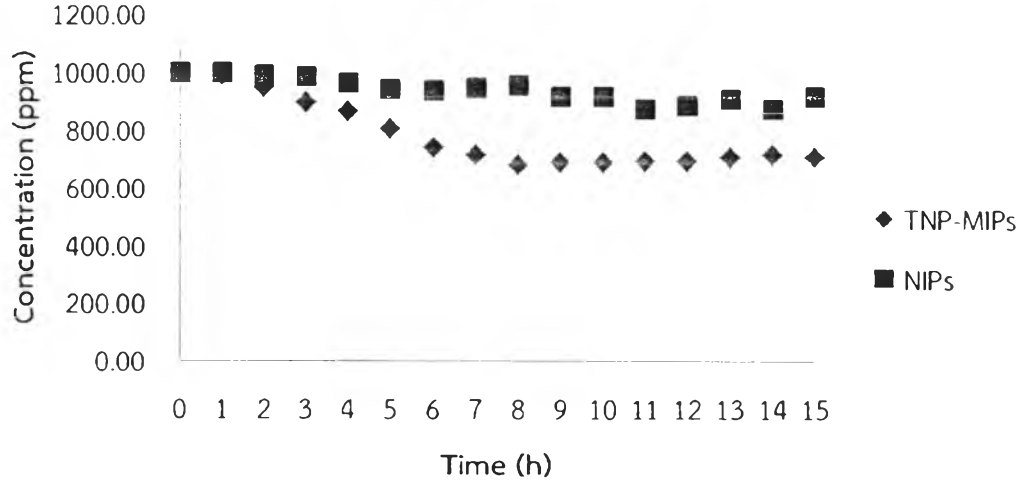

Figure 3.4 The concentrations of TNP in ethyl acetate solution in the presence of TNP-MIPs or NIPs at various times

To quantitatively compare the imprinting effect, we defined the specific adsorption values as:

$$\Delta Q = Q_{MIPs} - Q_{NIPs} \quad (1)$$

$$Q_{MIPs}\,(\mu mol/g) = \left(\frac{Ci\text{-}Ce}{W \times MW}\right) \times V \quad (2)$$

$$Q_{NIPs}\,(\mu mol/g) = \left(\frac{Ci\text{-}Ce}{W \times MW}\right) \times V \quad (3)$$

Where Ci and Ce are the initially measured concentration, and equilibrium concentrations (ppm) from the binding experiment, respectively. V (mL) is the volume of the solution. W (g) is the weight of the dried MIPs or NIPs used and MW is the molecular weight of the template molecules.

In the current experiment with TNP, we chose the Ce value at 8 h as the equilibrium point for the TNP-MIPs binding experiment, while the value for NIPs was

the average of the fluctuated values during 6-15 h of the NIPs binding experiment. The calculation **(Appendix B)** yielded the ΔQ values or the specific adsorption values of TNP molecules bound to the MIPs to be 128.41 μmol/g.

3.3.3 2,4,6-Trinitrotoluene-molecularly imprinted polymers (TNT-MIPs)

Similar binding experiments were performed for TNT-MIPs and similar trend of the results was observed. The concentration of TNT solution in ethyl acetate gradually decreased and reached equilibrium in 6 hours, slightly earlier than TNP-MIPs. The concentration of TNT solution in ethyl acetate for NIPs similarly showed no specific response to the template and started to fluctuate after 3 h **(Figure 3.5)**. Again, an obvious imprinting effect for TNT could also be noticed.

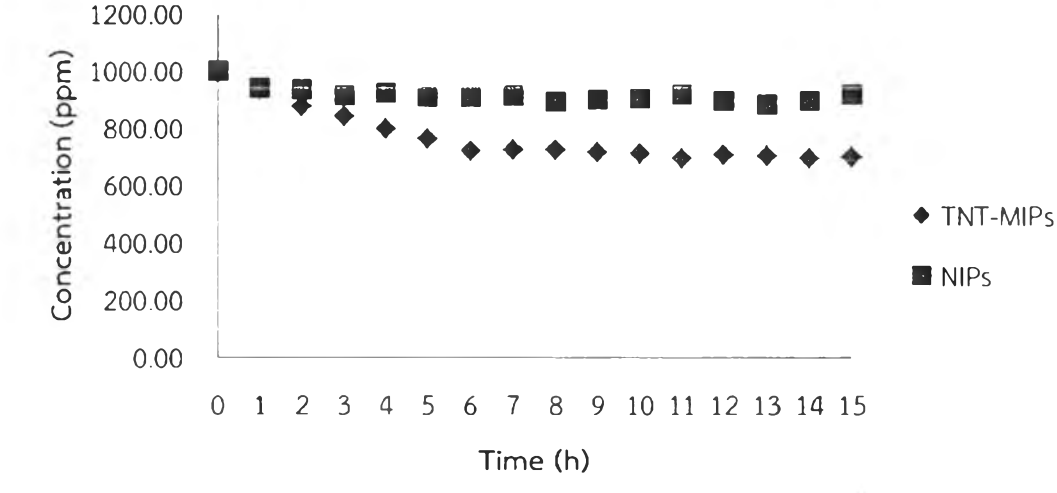

Figure 3.5 The concentrations of TNT in ethyl acetate solution in the presence of TNT-MIPs or NIPs at various times

In these experiments, the equilibrium concentration Ce was chosen to be at 6 h for the TNT-MIPs, while the value for NIPs was the average of the fluctuated values during 3-15 h of the NIPs binding experiment. The calculation **(Appendix B)** yielded the ΔQ values or the specific adsorption values of TNT molecules bound to the MIPs to be 103.63 μmol/g. The value is less than the previous case on TNP, perhaps suggesting less interactions of the template molecules to the polymer or less cavities created during the MIPs preparation.

Another method to determine the binding capacities of the MIPs was to estimate from the percentage of specific adsorption values from extraction the template off at the end of the binding process, compared to the initial amount of the template used to prepare the MIPs. The calculated binding capacities **(Appendix B)** were 38.64% for TNP and 28.63% for TNT, following the same trend as the earlier ΔQ calculations. The rather low numbers could be attributed to many factors. The bound template may not be completely extracted out of the MIPs with methanol. The initial concentration of the template used for the experiment may be too high compared to the actual rebinding capacities. It is also important to mention that the extracted TNP exhibited a red shift of the λ_{max} from 336 to 353 nm, indicating a change of the structure and related absorptivity and concentration.

3.4 Rebinding experiments

3.4.1 2,4,6-Trinitrophenol-molecularly imprinted polymers (TNP-MIPs)

MIPs and NIPs samples were further tested in rebinding processes using the same procedure as in binding experiments. The specific adsorption values (ΔQ) were calculated to prove the reusability of the MIPs. In this study, TNP-MIPs previously used in earlier experiments were exhaustively washed off the bound template before subject to rebinding experiments. The concentration of TNP solution in ethyl acetate in the presence of TNP-MIPs similarly decreased until steady after 5 hours. This equilibrium was reached sooner than the previous binding experiment and at much less absorption values, which was still distinguishable from those of NIP **(Figure 3.6)**.

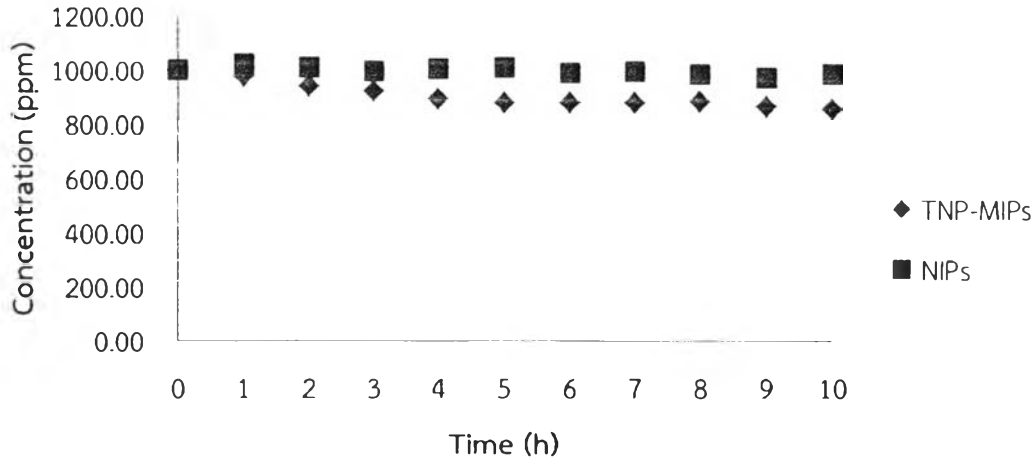

Figure 3.6 The concentrations of TNP in ethyl acetate solution in the presence of reused TNP-MIPs or NIPs at various times

For TNP rebinding experiment, the equilibrium concentration Ce was reached at 5 h for the TNP-MIPs, while the value for NIPs was the average of the fluctuated values during 3-10 h of the NIPs binding experiment. The calculation **(Appendix B)** yielded the ΔQ values or the specific adsorption values of TNP molecules bound to the MIPs to be 63.76 μmol/g. This rebinding capacity is only half of the first binding. Its large decrease indicated that the reused MIPs were much less efficient and not quite reusable, unfortunately.

3.4.2 2,4,6-Trinitrotoluene-molecularly imprinted polymers (TNT-MIPs)

Using the same condition of rebinding process for TNT-MIPs, the results of TNT-MIPs and its paralleled NIPs rebinding experiments were represented in **Figure 3.7.**

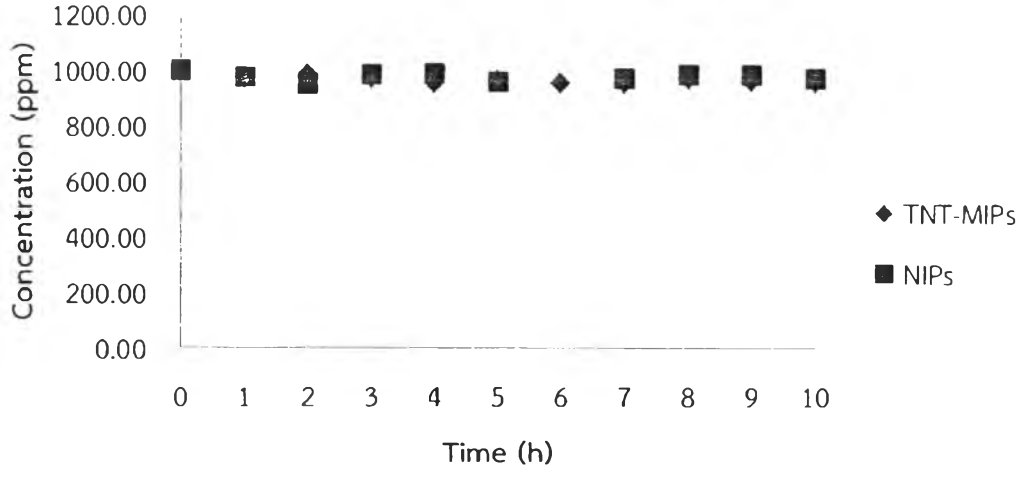

Figure 3.7 The concentrations of TNT in ethyl acetate solution in the presence of reused TNT-MIPs or NIPs at various times

For TNT rebinding experiment, the equilibrium concentration Ce was reached at 4 h for the TNT-MIPs, while the value for NIPs was the average of the fluctuated values during 2-10 h of the NIPs binding experiment. The calculation **(Appendix B)** yielded the ΔQ values or the specific adsorption values of TNT molecules bound to the MIPs to be only 12.37 μmol/g. This rather small value reinforced the earlier observation of irreusability of these materials. Especially in this case, the imprinting memory almost disappeared. Incomplete removal of the bound guest or further collapses of the imprinting cavities may be the reasons behind these disappointing results.

3.5 Cross binding experiment

To study whether the prepared TNP-MIPs and TNT-MIPs are selective to their respective imprinting molecules, the cross binding of mismatched template solutions were investigated. The exact binding experiment procedures were repeated using TNT added in TNP-MIPs, and TNP added in TNT-MIPs. The results of the cross binding experiments of TNP-MIPs and TNT-MIPs were shown in **Figure 3.8** and **3.9**, respectively. For comparison, the results from the binding experiments of the matched templates (**Figure 3.4** and **3.5**) were also included. The concentration of TNT solution in TNP-MIPs and TNP solution in TNT-MIPs both decreased slightly in

the beginning and later fluctuated, similar to non-selective binding experiments observed from NIPs. From these results, it was suggested that the prepared TNP-MIPs and TNT-MIPs had a high selectivity to its template molecules.

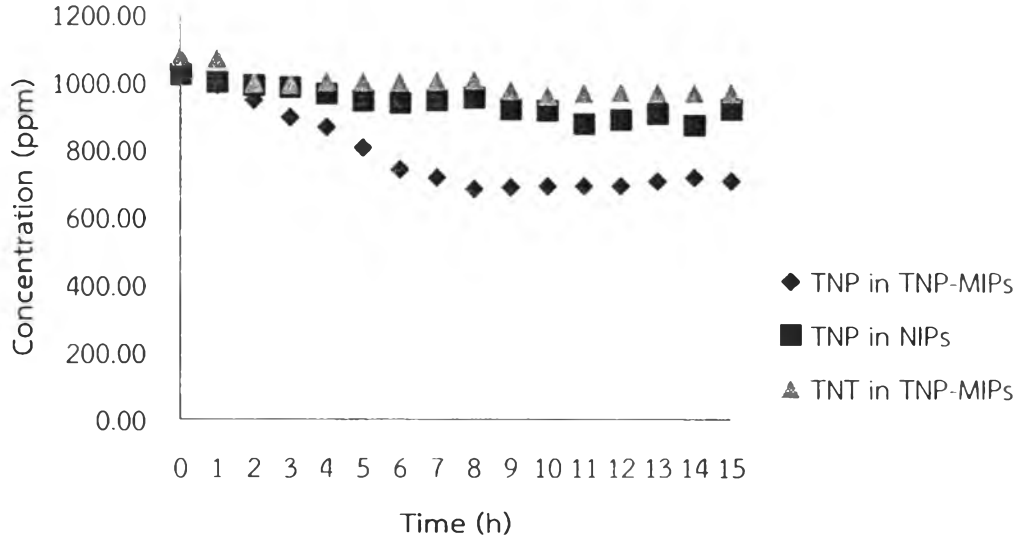

Figure 3.8 The concentrations of template solution in the presence of TNP-MIPs at various times

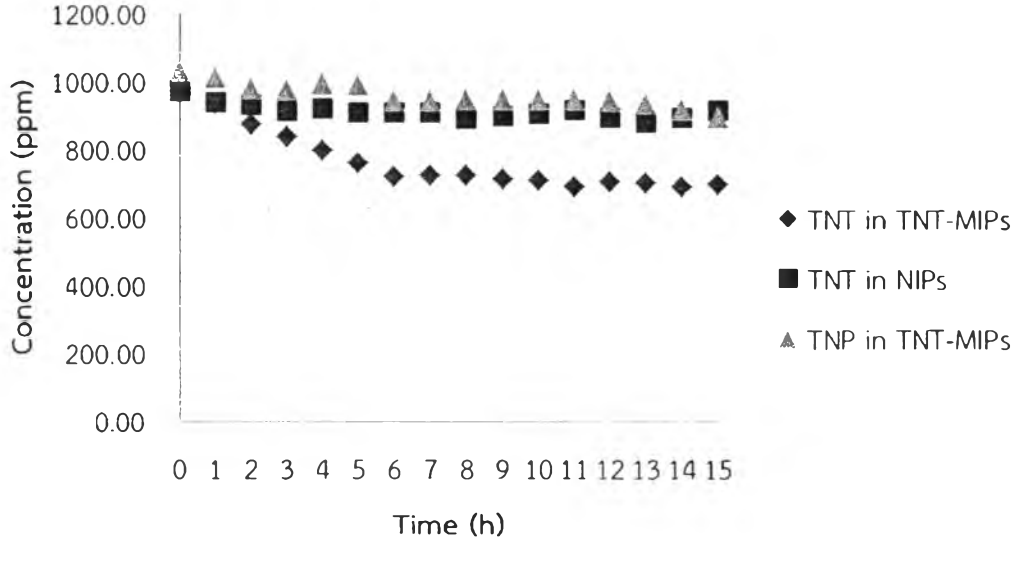

Figure 3.9 The concentrations of template solution in the presence of TNT-MIPs at various times